A high-content screen for small-molecule regulators of epithelial cell-adhesion molecule (EpCAM) cleavage yields a robust inhibitor

Received for publication, March 7, 2018, and in revised form, April 20, 2018 Published, Papers in Press, April 26, 2018, DOI 10.1074/jbc.RA118.002776

Jana Ylva Tretter[‡], Kenji Schorpp[§], Elke Luxenburger[¶], Johannes Trambauer[‖], Harald Steiner[‖], Kamyar Hadian[§], Olivier Gires[¶1,2], and Dierk Niessing[‡ ‡‡1,3]**

*From the [‡]Institute of Structural Biology and the [§]Assay Development and Screening Platform, Institute for Molecular Toxicology and Pharmacology, Helmholtz Zentrum München, German Center for Environmental Health, 85764 Neuherberg, Germany, the [¶]Department of Otorhinolaryngology, Head and Neck Surgery, Grosshadern Medical Center and the [‖]Biomedical Center, Metabolic Biochemistry, Ludwig-Maximilians-University Munich, 80539 Munich, Germany, the **German Center for Neurodegenerative Diseases, 81377 Munich, Germany, and the [‡‡]Institute of Pharmaceutical Biotechnology, Ulm University, 89081 Ulm, Germany*

Edited by Xiao-Fan Wang

Epithelial cell-adhesion molecule (EpCAM) is a transmembrane protein that regulates cell cycle progression and differentiation and is overexpressed in many carcinomas. The EpCAM-induced mitogenic cascade is activated via regulated intramembrane proteolysis (RIP) of EpCAM by ADAM and γ-secretases, generating the signaling-active intracellular domain EpICD. Because of its expression pattern and molecular function, EpCAM is a valuable target in prognostic and therapeutic approaches for various carcinomas. So far, several immunotherapeutic strategies have targeted the extracellular domain of EpCAM. However, targeting the intracellular signaling cascade of EpCAM holds promise for specifically interfering with EpCAM's proliferation-stimulating signaling cascade. Here, using a yellow fluorescence protein–tagged version of the C-terminal fragment of EpCAM, we established a high-content screening (HCS) of a small-molecule compound library (n = 27,280) and characterized validated hits that target EpCAM signaling. In total, 128 potential inhibitors were initially identified, of which one compound with robust inhibitory effects on RIP of EpCAM was analyzed in greater detail. In summary, our study demonstrates that the development of an HCS for small-molecule inhibitors of the EpCAM signaling pathway is feasible. We propose that this approach may also be useful for identifying chemical compounds targeting other disorders involving membrane cleavage-dependent signaling pathways.

The epithelial cell adhesion molecule (EpCAM)[4] is a calcium-independent homophilic cell adhesion molecule that belongs to the family of cellular adhesion molecules (CAM) (1). The *EPCAM* gene belongs to the tumor-associated antigen gene family GA-733 (2–4). Because EpCAM is overexpressed on a variety of carcinomas, it has been discovered numerous times by different groups and has been given various names. These names are based on the antibody or cDNA that were used for the identification of this antigen (5, 6). However, EpCAM is used as its primary name since 2007 (7). Up to now, a variety of functions of this protein have been described, ranging from cell adhesion (1, 8) to cell signaling that is involved in regulation of cell cycle and differentiation (9–16). Additionally, EpCAM is used as prognostic marker and therapeutic target in carcinomas (17–19).

In normal tissue, EpCAM displays a highly selective expression pattern in pluripotent embryonic stem cells (20, 21), hepatocytic progenitors (5, 22, 23), and epithelia (24). This expression is reactivated or enforced in the vast majority of carcinoma (25) and in cancer stem cells (26). The maintenance of the undifferentiated state of embryonic stem cells is strongly connected with EpCAM expression levels (6, 16, 20, 27). In carcinomas, EpCAM is highly overexpressed and (re-)distributed over the whole cell surface, which is frequently associated with cytoplasmic and nuclear staining (6, 28–31). In many cancer types, EpCAM overexpression is associated with a poor prognosis for the patient, *e.g.* lung, ovarian, and breast cancer, as well as pancreatic, gallbladder, and prostate carcinoma (18, 32–38). Exceptions to this are renal and thyroid carcinomas, in which high EpCAM expression is associated with an increased survival (30, 40). However, there are also cancer types such as gastric cancer in which the association of EpCAM expression with the outcome for patients was inconclusive (37). Recently, EpCAM was found to also be expressed on tumor cells of acute myeloid leukemia, with EpCAM-positive leukemic cells showing a greater resistance to chemotherapy (41).

EpCAM has a promoting role in cell proliferation. Several *in vitro* and *in vivo* studies demonstrated an induction of cell proliferation caused by EpCAM overexpression and a decreased cell proliferation after EpCAM down-regulation (9, 10, 14, 42). Induction of EpCAM expression leads to an up-regulation of the oncogenic transcription factor c-Myc, which eventually

This work was supported by Wilhelm Sander Foundation Grant 2015.019.1. The authors declare that they have no conflicts of interest with the contents of this article.

This article contains Tables S1–S3 and Figs. S1–S12.

[1] These authors contributed equally to this work.

[2] To whom correspondence may be addressed. E-mail: Olivier.Gires@med.uni-muenchen.de.

[3] To whom correspondence may be addressed. E-mail: niessing@helmholtz-muenchen.de.

[4] The abbreviations used are: EpCAM, epithelial cell-adhesion molecule; RIP, regulated intramembrane proteolysis; ICD, intracellular domain; EpICD, ICD of EpCAM; HCS, high-content screening; aa, amino acids; EpEX, extracellular domain of EpCAM; CTF, C-terminal fragment; YFP, yellow fluorescent protein; ANOVA, analysis of variance; h, human; PDL, poly-D-lysine.

results in up-regulation of cyclin A, D, and E (9, 14). Regulation of cyclin D1 expression was additionally demonstrated to occur through binding of the intracellular domain EpICD to consensus sequences of the *CCND1* promoter (14).

EpCAM is a 34–42-kDa type I membrane protein consisting of 314 aa and can be divided in three domains: a large extracellular domain (EpEX) of 242 aa, a transmembrane domain of 23 aa, and a short intracellular domain (ICD) of 26 aa (43–45).[5] The matured extracellular domain consists of an epidermal growth factor–like domain (aa 27–59), a thyroglobulin type 1A domain (aa 66–135), and a third cysteine-free motif that appears to be unrelated to any other known molecule (6, 46, 47). EpCAM is processed by regulated intramembrane proteolysis (RIP) (10), which is induced by juxtacrine signaling (48). Thereby, EpCAM molecules on two different cells interact with each other or with an as-yet-unknown ligand, which leads to the activation of RIP. The first step is a cleavage by ADAM proteases, in which EpEX is shed from the remaining C-terminal fragment (CTF = transmembrane domain + EpICD) of EpCAM (10, 49). Soluble EpEX can act as ligand for EpCAM, thereby enhancing the EpCAM signaling cascade in a paracrine way. Cleavage by membrane-associated α-secretases of the ADAM family is the prerequisite for the second step of RIP, which is conducted by γ-secretase (10). This subsequent step leads to the release of small, soluble extracellular fragments (EpCAM-Aβ-like) and the cytoplasmatic EpICD, which can vary in length because of differential cleavage (50). hEpICD is part of a large protein complex together with FHL2, β-catenin, and the transcription factor Lef-1 (10). This complex translocates into the nucleus and activates the transcription of EpCAM-target genes, which are genes involved in cell proliferation and growth, cell death, and reprogramming (9, 10, 14, 51–53). Via the interaction with FHL2 and its binding to β-catenin and Lef-1, EpCAM is linked to the Wnt pathway (52). Additionally, EpEX shedding can be conducted by the β-secretase BACE1 under acidic conditions, probably following endocytosis of EpCAM in acidified intracellular vesicles (50).

Because of its preferential strong expression in carcinomas, EpCAM is a suitable target for cancer therapy (6, 54). Therefore, EpCAM has been the target of different immunotherapeutic approaches, *e.g.* monoclonal antibodies, vaccination, and toxin- or tumor necrosis factor–related apoptosis-inducing ligand–conjugated antibodies (55–60). The first immunotherapeutic anti-EpCAM antibody was edrecolomab, which was produced in ascites of mice (61, 62). However, a clinical activity in adjuvant setting could not be confirmed (63, 64). In April 2009, the rat-mouse hybrid mAb catumaxomab (Removab®) was approved in the European Union for treatment of malignant ascites (65). Other EpCAM-directed antibodies are currently under development (6, 66). However, targeting of the intracellular EpCAM signaling cascade is an alternative and promising approach (67).

In the present study, we have addressed the development of inhibitors of EpCAM signaling through a high-content screening (HCS) approach. We established an automated, fluorescence-based imaging approach to investigate living cells with respect to alterations of cellular pathways upon administration of small inhibitory molecules. We subsequently performed an HCS with 27,280 compounds for the identification of hits that specifically inhibit the intracellular EpCAM signaling cascade. For the obtained hits, verification procedures and assessment of their toxicity and specificity toward EpCAM were established. One compound is described that shows significant effects on the intramembrane cleavage and thus signaling cascade of EpCAM. Hence, identification of small molecule inhibitors of EpCAM in the newly established HCS bears potential for the future development of inhibitory substances.

Results

Establishment of a high-content screen (HCS)

To establish a HCS for modulators of the EpCAM cleavage and signaling pathway, hEpCAM-negative human embryonic kidney HEK293 cells (9, 10) (Fig. S1*A*) were stably transfected with a plasmid expressing a fusion of the preactivated C-terminal fragment of EpCAM with yellow fluorescent protein (hEpCAM–CTF–YFP). This fusion protein allows for the spatial detection of EpCAM-cleavage products in different compartments of the cell (Fig. 1, *A* and *B*). Treatment of cells with a compound that affects the intramembrane cleavage and/or signaling of EpCAM should result in an accumulation of YFP fluorescence in specific cellular compartments such as the membrane, the cytoplasm, or the nucleus (Fig. 1*B*). As control, fluorescence intensities in subcellular compartments of compound-treated cells were referred to intensities in DMSO-treated cells. If the compounds gave ~50% more YFP signal intensity in one of the four cell regions (nucleus, ring (*i.e.* cytoplasm), membrane and/or cell) as obtained in the DMSO solvent control and if the number of selected cells per well exceeded a predefined threshold (>20 nuclei selected per well), this compound was regarded as a hit.

Fluorescence intensities in each subcellular compartment were calculated using the Columbus High-Content Imaging and Analysis Software and included several sequential steps (Fig. 1*C*). To allow the automated software to distinguish between different compartments, the nucleus was stained with Hoechst 3342, and the cell membranes were stained with the Cell Mask dye. In the first step, all cells were identified by their nuclear Hoechst 3342 staining. Subsequently, all cells that did not meet certain imaging criteria regarding roundness and area (for details see "Experimental procedures") were excluded from further analysis (selection of population; Fig. 1*C*). During subsequent steps, the cytoplasm of each cell was selected, and thereafter the nucleus, cytoplasm, and membrane regions were defined, and the YFP intensities were assessed. The value of the calculated YFP intensity in each region was normalized to the size of the region and to the number of the analyzed cells (Fig. 1*C*). For the identification of small molecule inhibitors targeting the intracellular EpCAM signaling cascade, a suitable HCS setting had to be established. Hence, optimal conditions for imaging (magnification and imaging method), staining of the cells and optimal cell number per well had to be determined. Therefore, HEK293 hEpCAM–CTF–YFP cells were treated

[5] Please note that the JBC is not responsible for the long-term archiving and maintenance of this site or any other third party hosted site.

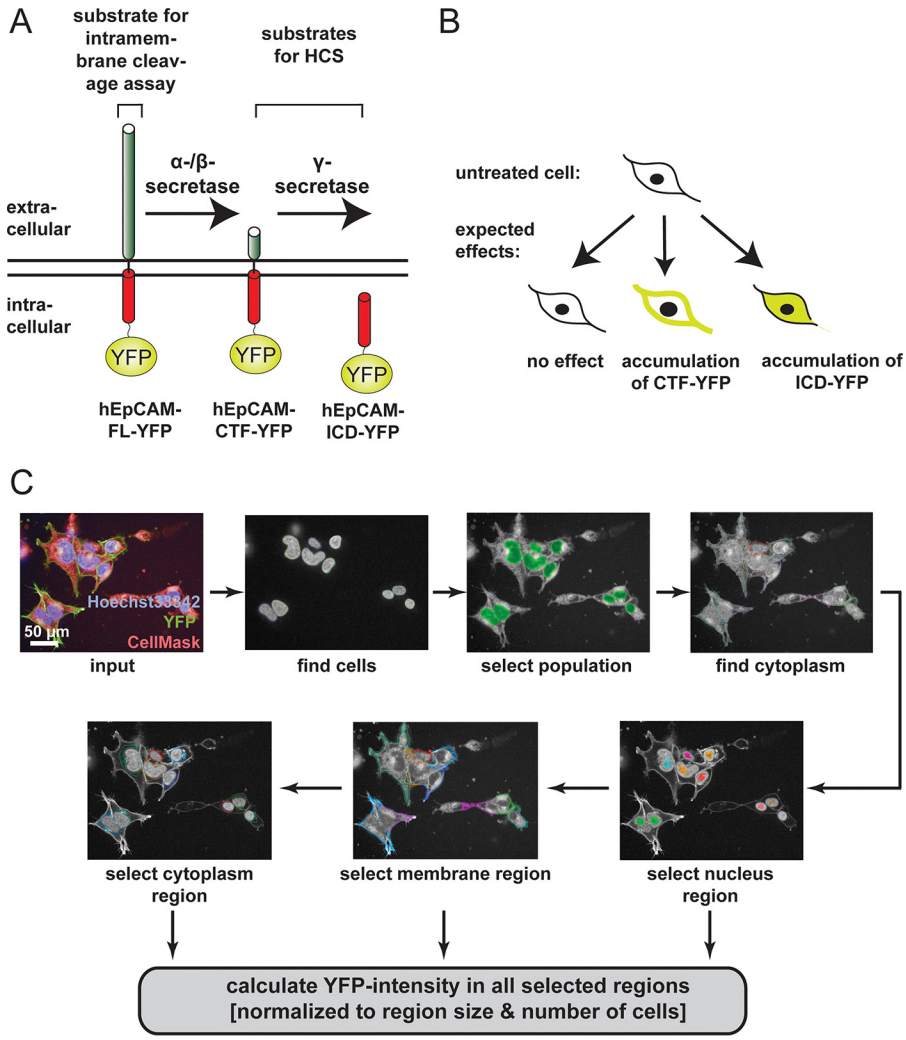

Figure 1. Principle of HCS and image analysis. *A*, different C-terminally YFP-fused hEpCAM fragments are depicted. hEpCAM–CTF–YFP is generated by α-/β-secretase cleavage of hEpCAM–FL–YPF. Subsequent cleavage of hEpCAM–CTF–YFP leads to formation of EpICD–YFP. hEpCAM-FL-YFP is the construct used for intramembrane cleavage assays. hEpCAM–CTF–YFP and EpICD–YFP are the fragments relevant for HCS. *B*, possible effects of compound treatment. Small molecules could either have no effect (*left*), lead to accumulation of hEpCAM–CTF–YFP at the membrane (*middle*), or to accumulation of hEpCAM–ICD in the cytoplasm or nucleus (*right*). *C*, image analysis. After selection of the cells that are included in the downstream analysis, the different cell regions are defined, and the YFP intensities for each region are calculated.

with the γ-secretase inhibitor DAPT, which inhibits cleavage of hEpCAM–CTF–YFP (10) and thereby leads to stabilization and accumulation of this fragment at the cell membrane, resulting in a significant increase of YFP fluorescence at the cell membrane. After this treatment, the cells were stained and imaged under different conditions regarding imaging methods (confocal *versus* nonconfocal), magnification (40× *versus* 60×), cell density (3,000 *versus* 5,000 cells/well) and staining (DRAQ5 *versus* CellMask), evaluated, and compared, and the optimum conditions were chosen for performing the HCS (Fig. S1*B*). To streamline the screening procedure, three areas of each well were imaged instead of entire wells. Analysis revealed 40× magnification with 3,000 cells/well and CellMask staining to be optimal for the HCS (Fig. S1*B*). When comparing results of confocal imaging and nonconfocal imaging, it could be shown that confocal imaging facilitates significant differentiation between the cell regions regarding YFP intensities (Fig. S1*B*).

Performance of HCS and first validation of hits

The initial screen was performed with 27,280 small molecules at a final concentration of 8 μM. DMSO and DAPT (10 μM) were used as negative and positive control, respectively. HEK293–hEpCAM–CTF–YFP cells (Fig. 1, *A* and *C*) were automatically seeded onto 384-well plates, treated with the compounds, stained, and fixed, and the effects of the compound treatment on the cells were analyzed (Fig. 2*A*). For every initial screening plate, the Z′ score (71) was calculated for every subcellular compartment (membrane region, cytoplasm, nucleus, and YFP total). If at least the Z′ score for one region was between 0.3 and 1.0, the respective screening plate was included in further analysis (Fig. S2). After initial screening and analysis, 128 compounds were identified as primary hits (hit rate, 0.45%). These hits were reanalyzed in a 5-point titration (80–5 μM), in which 81 compounds showed a reproducible effect and were thus confirmed (Fig. 2*B*). Afterward, 81 molecules were reordered and tested in a 10-point titration (80–0.15 μM), by which

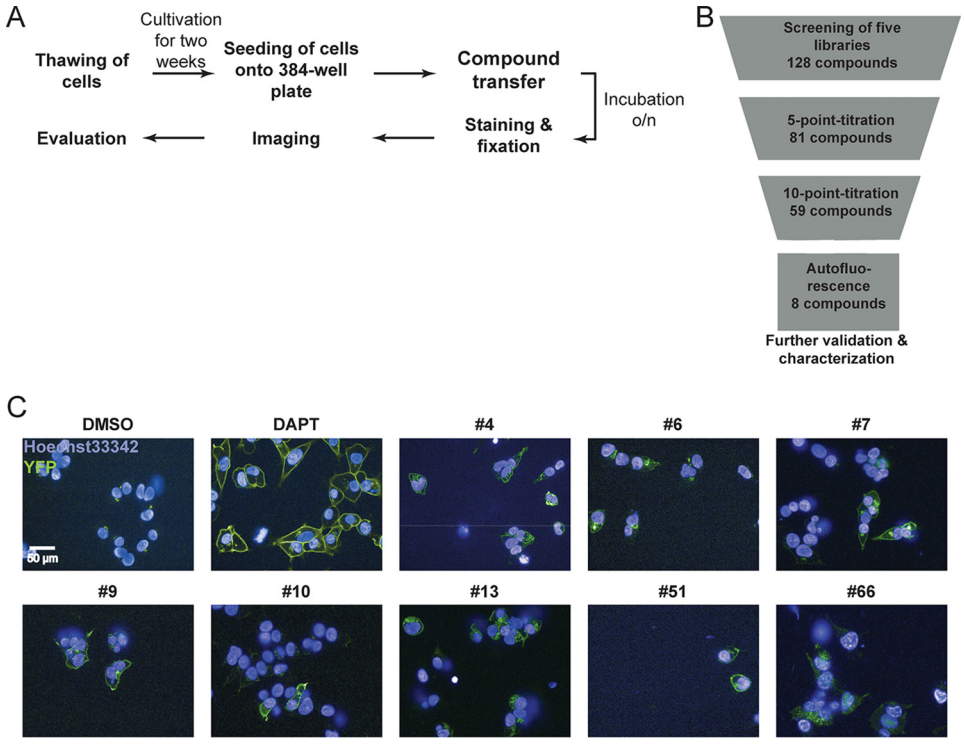

Figure 2. Performance and results of HCS. *A*, overview of HCS process. The cells were cultivated and automatically seeded onto 384-well plates. Compounds were transferred and incubated overnight before cells were stained, fixed, and finally imaged. *B*, summary of hit validation. Shown are the number of remaining compounds as well as the reason for exclusion of others. *C*, images of the effects of the remaining eight compounds on the cells. Treatment with DMSO shows no effect, whereas DAPT led to accumulation of hEpCAM–CTF–YFP (*green*) at the membrane. Seven compounds also led to accumulation of hEpCAM–CTF–YFP at the membrane. Compound 66 led to accumulation in the cytoplasm. The compound number is given *above* the respective image. The nuclei are stained with Hoechst 33342 (*blue*). For a better visualization of the corresponding effects, CellMask staining is not shown in these images. The *scale bar* represents 50 μm. Pictures of compounds were taken with autocontrast function.

59 compounds could be confirmed. Because the readout of the screen was fluorescence, it was important to exclude false-positive results arising from autofluorescence of compounds. Therefore, YFP-lacking HEK293–hEpCAM–CTF cells were treated with the respective compounds, and their fluorescence signal was analyzed. As a result, 51 additional compounds were excluded because of autofluorescence (data not shown) (Fig. 2*B*). Of the remaining eight compounds, seven showed accumulation of CTF–YFP at the membrane, and compound 66 showed accumulation of EpICD–YFP in the cytoplasm (Fig. 2*C*). These compounds were considered as high-confidence hits and studied further with regards to toxicity, effects on intramembrane cleavage of hEpCAM, effects on the transcriptional level of EpCAM target genes, and effects on cell proliferation.

Cytotoxicity of compounds

Because general cytotoxicity of a compound is detrimental to its use as potential drug, we assessed the effects of the eight compounds on viability, cytotoxicity, and apoptosis. To find a potential EpCAM-specific effect, four different EpCAM-positive and -negative cell lines were used. These are EpCAM-negative HEK293 WT cells, HEK293–hEpCAM cells, and two endogenously EpCAM-expressing cell lines: HCT-8 cells and FaDu hypopharynx cells. These cell lines were automatically seeded onto 384-well plates, treated with the verified hits from our screen with the drug staurosporine as positive control (80–0.15 μM) or DMSO (negative control), and analyzed after 16 h of incubation. The results were related to DMSO as a control (Fig. 3*A*). In none of the cases did we observe cell-type–specific differences in viability, cytotoxicity, or apoptosis. Staurosporine expectedly led to a strongly decreased viability (−) and strongly increased cytotoxicity and apoptosis (++). Compound 7 did not show any effects on the cells, whereas compounds 13 and 66 strongly impaired cell viability. Compounds 4, 6, 9, 10, and 51 had only minor effects on the cells (for a detailed presentation of the results, see Figs. S3–S7).

Effects of compounds on regulated intramembrane cleavage

The effect of high-confidence hits on regulated intramembrane proteolysis of full-length hEpCAM (Fig. 1*A*) was analyzed in membranes isolated from HEK293–hEpCAM–YFP cells. Following preincubation of cells with the indicated compounds/inhibitors, membrane fractions were isolated. To assess substrate cleavage, membrane fractions were incubated at 37 °C for 22 h in the presence of newly added compounds/inhibitors. DMSO was used as vehicle control. Cleavage products were analyzed in immunoblot experiments using anti-GFP antibodies (which recognizes YFP). After 22 h of incubation without inhibitor or with DMSO, hEpCAM–YFP (66 kDa) was cleaved into the membrane-associated CTF–YFP (35 kDa) and the soluble ICD of EpCAM (hEpICD–YFP; 31 kDa) (Fig. 3*B*, *top panel*). Incubation with the ADAM protease inhibitor GI254023X and β-secretase inhibitor (C3) led to inhibition of cleavage of hEpCAM–YFP. This inhibits the formation of hEpCAM–CTF–YFP but still allows for the cleavage of already

A

Compound No.	Viability	Cytotoxicity	Apoptosis
DMSO	0	0	0
staurosporine	--	++	++
#4	0	0	+
#6	-	+	+
#7	0	0	0
#9	-	0	0
#10	-	0	0
#13	--	++	+
#51	0	0	+
#66	--	+	--

B

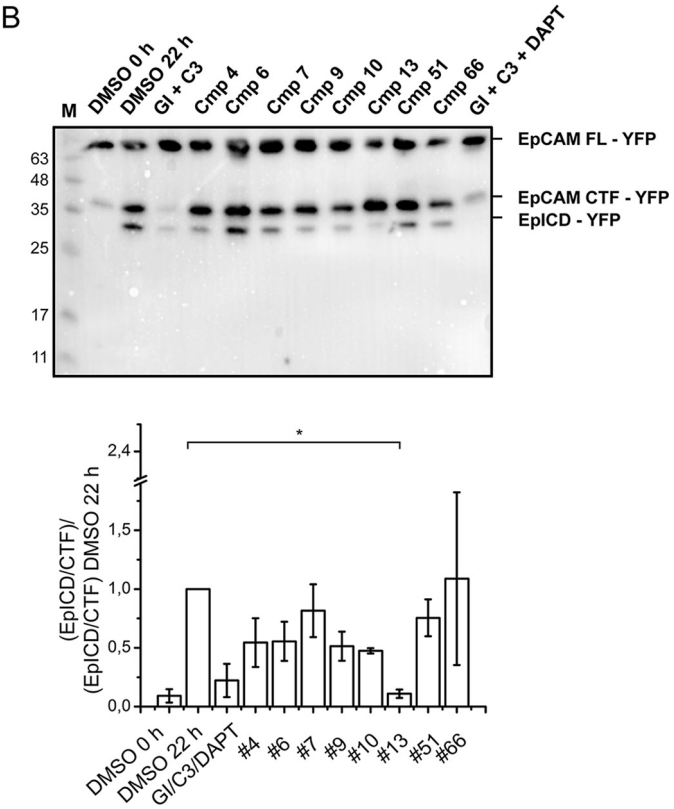

Figure 3. Effects on viability and intramembrane cleavage. *A,* HEK293 WT, HEK293 hEpCAM-FL, HCT-8, and FaDu cells were treated with compounds, DMSO, or the drug staurosporine as control. Effects on cell viability, toxicity, and apoptosis are summarized in the table. The data for each cell line are summarized in Figs. S3–S7 *B,* HEK293 hEpCAM–CTF–YFP cells were treated as indicated. Isolated membrane fractions were separated in SDS–PAGE, and cleavage products were detected by a GFP-specific antibody (recognizes YFP equally well). Shown is one representative blot of three experiments (*top panel*). In the *bottom panel*, the ratio of the intensities of EpICD–YFP/EpCAM–CTF–YFP bands were compared with EpICD/CTF ratio of DMSO 22-h control. Shown are mean values and standard deviations of three independent experiments. Compound 13 led to a highly significant decrease of EpICD/CTF. Statistical significance was verified using one-way ANOVA. *p* values are given above *bracket* (*bottom panel*). *, $p < 0.0004$.

formed fractions of this fragment into hEpICD–YFP (Fig. 1*A*). ADAM/BACE inhibition in conjunction with the γ-secretase inhibitor DAPT abrogated hEpICD–YFP formation (Fig. 3*B*, *top panel*). The effects of compounds on EpCAM cleavage were quantified from Western blots ($n = 3$ independent experiments) by calculating the ratios of the intensities of hEpICD–YFP/CTF–YFP bands relative to EpICD/CTF DMSO 22-h control. Compounds 4, 6, 9, 10, and 13 show a reduced signal. However only compound 13 significantly decreased hEpICD–YFP intensity (0.11 ± 0.04) when using the strict one-way ANOVA analysis with Bonferroni correction (Fig. 3*B*, *bottom panel*). Compound 13 did not significantly impede CTF formation, which indicates that this compound has an influence on γ-secretase–mediated cleavage of the CTF fragment of full-length EpCAM (Fig. 3*B*, bottom panel). For details of one-way ANOVA, see Table S1.

Effects on EpCAM target gene transcription

For the investigation of a possible effect of compound treatment on EpCAM target gene transcription, the expression level of *CCND1* (cyclin D1) was assessed. To define an EpCAM-specific effect on proliferation, HCT-8 colorectal adenocarcinoma WT and a CRISPR-Cas9-mediated *EPCAM* KO clone of HCT-8 cells (50) were tested, and the results were compared. Inhibition of EpICD formation through treatment with DAPT resulted in an average of 13% reduction of CCND1 transcript levels in $EpCAM^+$ HCT-8 cells, but not in EpCAM–KO HCT-8 cells (Fig. 4*A*). Further analysis of relative expression levels revealed a significant decrease after treatment with compounds 4, 6, 9, 10, 13, 51, and 66 in HCT-8 WT cells (Fig. 4*A*, *left panel*; $p < 0.05$). In HCT-8 KO cells, compounds 4 and 6 led to a significant decrease of *CCND1* expression level (Fig. 4*A*, *right panel*; $p < 0.05$), suggesting an EpCAM-independent effect. Comparison of expression levels in WT cells and in KO cells showed that compound 10 led to statistically significant reduction of *CCND1* exclusively in HCT-8 WT cells, which indicates an EpCAM-specific effect.

Effect on proliferation of cells

To address a potential EpCAM-specific effect of the compounds on cell proliferation, HCT-8 WT and EpCAM–KO cells were treated with compounds DAPT or DMSO. Over a period of 7 days, cell numbers were determined on a daily basis, using the automated Operetta Imaging System. None of the compounds showed a significant difference between EpCAM-positive and -negative cells. Compound 66 did not show an effect on cell proliferation. Compounds 9, 10, and 7 had minor effects on the proliferation of HCT-8 WT and KO cells. Compounds 4, 6, 13, and 51 almost completely inhibited cell proliferation of both cell lines at the given concentration (Fig. 4, *B* and *C*).

Screening of analogs

Based on the results of the membrane-cleavage assays and similarities in chemical scaffolds, analogs of compounds 4, 9, 10, and 13 were selected. In total, 39 new compounds were assessed: 13 analogs of compound 4, 4 analogs of compound 9, 13 analogs of compound 10, and 9 analogs of compound 13 were chosen. These compounds were compared with the original compounds in a 10-point titration (80 – 0.15 μM) with the primary screening assay in HEK293– hEpCAM–CTF–YFP cells (data not shown). The effects of all compounds were visually assessed regarding their efficiency and toxicity. If an analog showed comparable or better effect with simultaneously less toxicity, this compound was used for further studies. Furthermore, an assessment of the analogs using HEK293– hEpCAM cells showed no autofluorescence for any of them (data not shown). In summary, 9 of 39 analogs were chosen for further studies (Fig. 5).

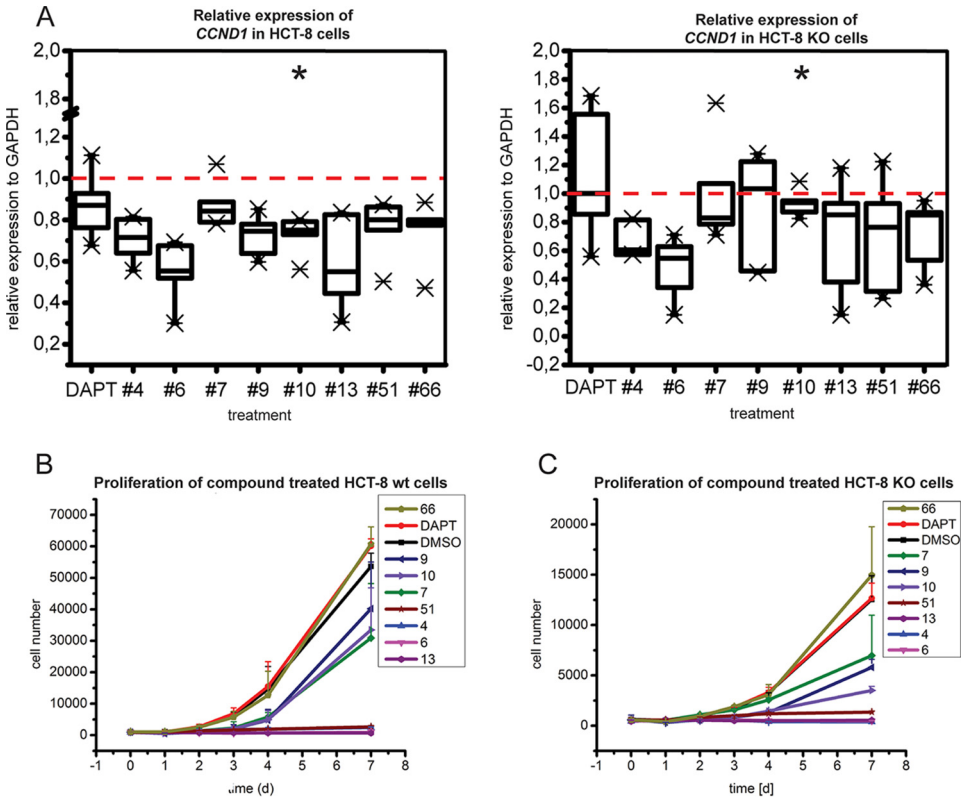

Figure 4. Effects on target gene expression and cell proliferation. *A*, effects on *CCND1* expression was assessed with EpCAM-positive HCT-8 WT cells (*left panel*) and EpCAM-negative HCT-8 KO cells (*right panel*). Compounds 4, 6, 9, 10, 13, 51, and 66 showed an effect in WT cells, and compounds 4 and 6 showed an effect in KO cells. Compound 10 yielded a significant, EpCAM-specific down-regulation of *CCND1* expression. Shown is the evaluation of five independent experiments. *Whiskers* span the 10–90 percentiles. Statistical analysis was performed using paired-sample *t* test. *p* values of *t* tests between the cell lines are depicted by an *asterisk*. *, $p < 0.01$. The *red dashed lines* show DMSO as reference. *B* and *C*, HCT-8 WT and EpCAM–KO cells were plated and treated with compounds, and cell numbers were determined on a daily basis. No difference could be detected between the two cell lines. Compounds 4, 6, 13, and 51 strongly impaired cell proliferation; compounds 7, 9, and 10 had minor effects, whereas compound 66 did not show any effect.

Cytotoxicity of analogs

To test the toxicity characteristics of the original compounds and the nine analogs, their effects on the viability of cells were tested. Therefore, different EpCAM-positive and -negative cell lines were treated with DMSO, staurosporine (positive control) or compounds and analyzed after 16 h of incubation (Fig. 6*A*). There were no observable differences in viability, cytotoxicity, and apoptosis between EpCAM-positive and -negative cell lines. Remarkably, none of the analogs of compound 13 showed any toxic effect on the cells, whereas the original compound 13 showed a strong reduction in viability (two independent experiments with three replicates each; compare Fig. 6*A* with Fig. 3*A*; Figs. S8–S12). Thus, analogs of 13 have an improved toxicity profile.

Effects of analogs on intramembrane cleavage of hEpCAM

The effect of the selected nine analogs on hEpCAM cleavage was analyzed on isolated membranes of HEK293–hEpCAM–YFP cells. As before, the ratio of the intensities of the HEpCAM–CTF–YFP/hEpICD–YFP bands was calculated relative to the CTF/EpICD DMSO 22-h control (Fig. 6*B*). Compound 13_1 (0.33 ± 0.07) and 13_7 (0.36 ± 0.14) showed a significant decrease of CTF/EpICD–YFP intensity, but these effects were no improvement when compared with the original compound 13 (0.11 ± 0.04) (Fig. 3*B*). In contrast to the primary hits 9 and 10, the analogs 9_0 (0.29 ± 0.12), 10_4 (0.57 ± 0.08), 10_6 (0.26 ± 0.07), 10_9 (0.38 ± 0.16), 10_10 (0.3 ± 0.09), and 10_12 (0.29 ± 0.01) reduced significantly the CTF/EpICD–YFP intensity, which also indicates an influence on γ-secretase cleavage for these compound series. For the remaining analog 4_7, no significant, reproducible effects were observed. For details of one-way ANOVA, see Table S2.

Effects of analogs on EpCAM target-gene transcription

For the investigation of a possible effect of the analogs on EpCAM-dependent *CCND1* expression, HCT-8 WT and KO cells were treated with DMSO (control) or analogs of compound 10. Our analysis was restricted to analogs of compound 10 because this compound was the only one that showed an EpCAM-specific effect (Fig. 4*A*). In WT cells, compounds 10_4 and 10_12 showed a significant decrease of *CCND1* expression (Fig. 7*A*, *left panel*; $p < 0.05$). In KO cells, only compound 10_12 showed a significant effect (Fig. 7*A*, right panel; $p < 0.01$). Comparison of expression levels in WT and KO cells showed that compound 10_12 led to significant reduction of *CCND1* in HCT-8 WT cells (Fig. 7*A*). In summary, these findings indicate that only compound 10_4 has a modest but EpCAM-specific effect.

Effects of compound 10 and analogs on cell proliferation

To confirm potential EpCAM-specific effects of compound 10 analogs on cell proliferation, HCT-8 WT and -KO cells were treated with analogs, DAPT, or DMSO as control. The cell

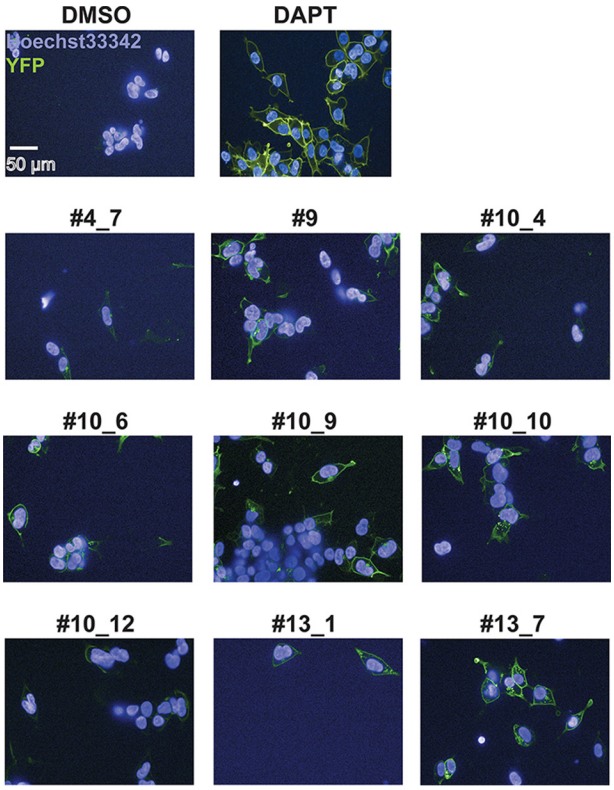

Figure 5. Effects of nine selected analogs on HEK 293 hEpCAM–CTF–YFP cells. Treatment with DMSO shows no effect, whereas DAPT led to accumulation of hEpCAM–CTF–YFP (*green*) at the membrane. All shown analogs led to accumulation of hEpCAM–CTF–YFP at the membrane and improved efficiency or lower toxicity. The compound number is given *above* the respective image. The nuclei are stained with Hoechst 33342 (*blue*). CellMask staining is not shown to allow for a better recognition of effects. The *scale bar* represents 50 μm. Pictures of compounds were taken with autocontrast.

A

Compound No.	Viability	Cytotoxicity	Apoptosis
DMSO	0	0	0
staurosporine	--	++	++
#4_7	-	+	0
#9	0	0	0
#10_4	-	0	0
#10_6	-	0	0
#10_9	0	0	0
#10_10	-	0	0
#10_12	-	0	0
#13_1	0	0	0
#13_7	0	0	0

B

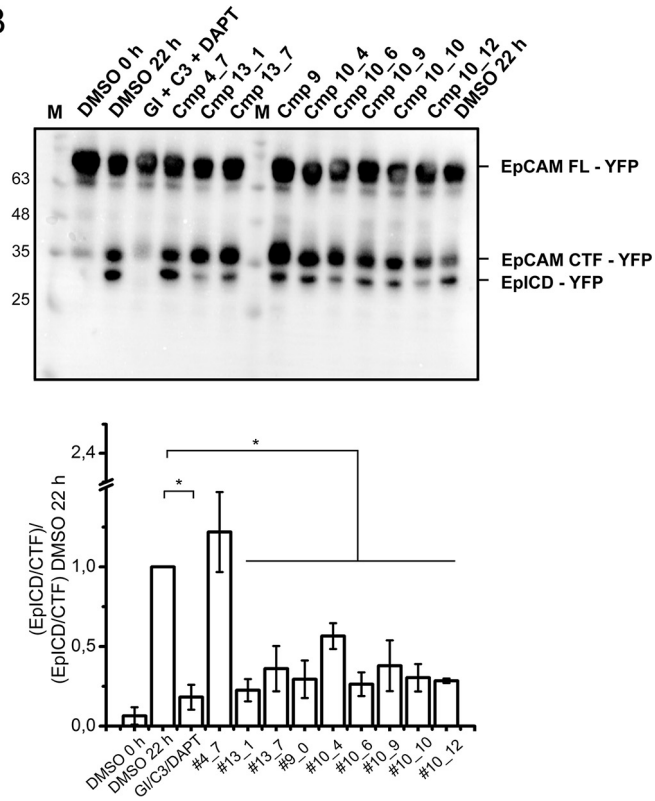

Figure 6. Effects on viability and intramembrane cleavage. *A*, HEK293 WT cells, HEK293 hEpCAM-FL cells, HCT-8, and FaDu cells were treated with compounds, DMSO, or the drug staurosporine as control. Effects on cell viability, toxicity, and apoptosis are summarized in the table. No compound showed an effect on cell viability. *B*, HEK293 hEpCAM–CTF–YFP cells were treated as indicated. Isolated membrane fractions were separated by SDS–PAGE, and cleavage products were detected using an YFP-specific antibody. Shown is one representative blot of three (*left panel*). Evaluation was done as described above. Shown are mean values and standard deviations of three independent experiments. Compounds 13_1, 13_7, 10_4, 10_6, 10_9, 10_10, and 10_12 led to a significant decrease of EpICD/CTF signal. Statistical significance was verified using one-way ANOVA. *p* values are given above brackets (*right panel*). *, $p <$ 0.0004.

numbers were automatically counted every 24 h for a total duration of 7 days. No difference could be seen between HCT-8 WT and HCT-8 EpCAM KO cells for any compound. Additionally, none of the analogs of compound 10 showed significant effects on cell proliferation (Fig. 7*B*).

Discussion

EpCAM signaling based on RIP is an attractive target for potential small molecule inhibitors, which might be effective in carcinoma cells. The rationale for this approach relies on the strong overexpression of EpCAM primarily in cancer cells and an apparently preferential RIP-dependent cleavage in tumor cells (10). In fact, most recent data suggest that signaling through EpICD does not impact proliferation of normal liver cells (22), whereas EpICD regulates gene expression and tumor progression in hepatocellular carcinomas (39). To identify potential inhibitors of EpCAM cleavage, we have successfully established a HCS using the precleaved and highly reactive C-terminal fragment of EpCAM in a YFP-fused version.

This HCS yielded robust (Z scores between 0.5 and 0.9; Fig. S2) and reproducible results. Effects seen in the initial screen could be reconfirmed in hit picking campaigns with the same compounds, as well as with newly ordered compounds. An advantage of the here-performed HCS is that by measuring an increase in YFP fluorescence in a specific subcellular compartment, possible modes of actions of the hits can already be anticipated. Therefore, further characterization of a given hit compound and its effect can be done in a more targeted way. In the here-performed screen, seven compounds showed accumulation of YFP at the membrane. Based on this information, we performed membrane assays that confirmed that these compounds indeed affect γ-secretase cleavage of EpCAM.

After investigating the effects of the eight high-confidence hits on cell viability, proliferation, target gene expression, and regulated intramembrane proteolysis, four compounds showed promising results: compounds 4, 9, 10, and 13. Therefore, ana-

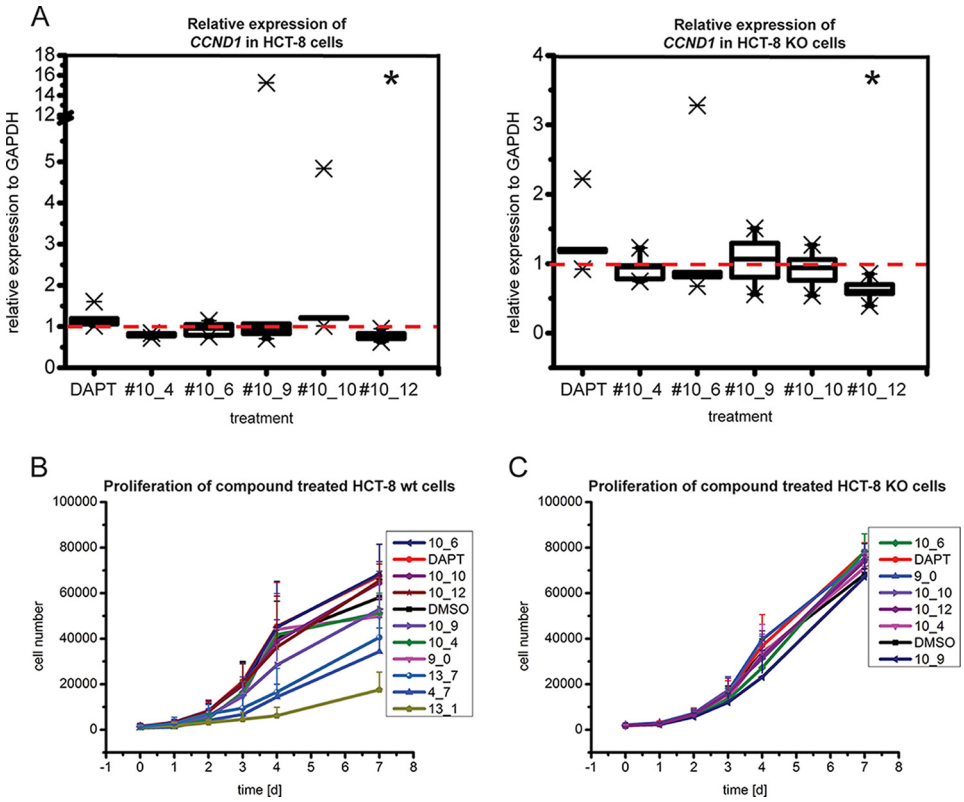

Figure 7. Effects on target gene expression and cell proliferation. *A*, effects on *CCND1* expression was assessed by quantitative RT–PCR with EpCAM-positive HCT-8 WT cells (*left panel*) and EpCAM-negative HCT-8 KO cells (*right panel*). Compounds 10_4 and 10_12 showed an effect in WT cells, and only compound 10_12 showed an effect in KO cells. Shown is the evaluation of five independent experiments. *Whiskers* span the 10–90 percentiles. Statistical analysis was performed using paired-sample *t* test. *B* and *C*, HCT-8 WT and KO cells were plated and treated with compounds, and the cell number was determined daily. Compound 13_1 strongly impaired cell proliferation, and compounds 4_7 and 13_7 only had minor effects on the proliferation of WT cells. All other compounds did not have an effect on cell proliferation, and none of the analogs of compound 10 showed an EpCAM-specific effect. The *red dashed lines* show DMSO as reference.

logs of these compounds were chosen and investigated under the same conditions as before, which allowed us to analyze the structure–activity relationship (a summary of all compound structures is found in Table S3). For the efficacy of compound 4, a 2-methoxysubstitution on the right-hand aromatic ring seemed to be crucial. If this substitution is in any other position, the compound lost its efficacy (*e.g.* compounds 4_2 and 4_5). The fluorine-derivatized compounds showed a very weak effect (4_3 and 4_4). The only alternative is a chloride instead of a methoxy substitution; however, this compound 4_6 was more toxic than 4 and less effective. Compounds 4_7 and 4_9 have a chlorine and fluorine substitution at the left aromatic ring, respectively. Additionally, they show a benzyl-cycloalkylamin at the right aromatic ring. The cycloalkyl seemed to be important, because derivatives without this residue do not have any effect (*e.g.* 4_10 and 4_13). The structures of compound 9 and 10 have a very similar scaffold. The basic backbone consisting of a 2 + 1 ring system is consistent and only altered by differential substituents. It seems that a secondary amine (R1-NH-R2) has a somewhat better efficacy than N-substitution. For analogs of 13_0, it was shown that a benzyl group drastically reduces cytotoxicity but shows comparable effectiveness (13_1). Moreover, compounds substituted at the exo-N (13_5 to 13_9) also show similar effects and toxicity as the analogs, which are substituted at the N within the aromatic ring. The benzyl group reduces the cytotoxicity of these compounds as well. In general, compounds 4 and 13 are structurally similar in that they show the same basic backbone, except for compound 13 having an oxygen atom instead of sulfur atom in the five-membered ring. All benzyl-substituted derivatives show the best effects and additionally decrease cellular toxicity for analogs of compound 13.

The five-point and ten-point serial dilutions were performed with compounds from stock aliquots and newly provided by the supplier, respectively. In some cases, the effect shown in the initial HCS campaign was not reproducible. Several reasons might account for this. Because the compounds for HCS were stored in multiwell plates in DMSO at −20 °C, freeze-thaw cycles might have led to degradation of the compounds and thus changing efficiency. Thus, in some cases a degradation product might have been the cause of inhibitory effects observed in the initial screen. Moreover, newly provided compound samples might differ in their purity and identity of possible contaminants.

In summary, in this study we have established a robust and reliable HCS for inhibitors and identified compounds that affected the membrane cleavage of EpCAM. Our work demonstrates the feasibility of a HCS against EpCAM signaling pathway that is potentially also applicable for other disorders involving membrane cleavage– dependent signaling pathways.

Experimental procedures

Cell lines

Human embryonic kidney cells (HEK293), human colon carcinoma cell line HCT-8,, and human hypopharyngeal carci-

noma cell line FaDu were cultivated in Dulbecco's modified Eagle's medium with 10% fetal calf serum, 1% Fungizone, and 1% penicillin/streptomycin. All cell lines were grown in a 5% CO_2 atmosphere at 37 °C. HCT-8 CRISPR-Cas9-mediated EpCAM KO clones were prepared by T. Tsaktanis as previously described (50). All cell lines have been confirmed by STR-typing at the Helmholtz Zentrum München.

Transfections and expression vectors

Transfections were performed using the MATra reagent (Iba, Goettingen, Germany) according to the manufacturer's instructions. Stable selection of transfectants was done by using puromycin (1 μg/ml) in the culture medium starting at day 1 after transfection. Human EpCAM (hEpCAM) full-length (314 aa) was cloned without YFP. The CTF mimic of hEpCAM termed hEpCAM–CTF–YFP consists of a signal peptide sequence MPRLLTPLLCLTLLPALAARGLR, a Myc tag (EQKLISEEDL), CTF sequence of hEpCAM (251–315), FLAG tag (DYKDDDDK), the TEV recognition site (ENLYFQG), and YFP. The constructs were cloned into the 141 pCAG-3SIP expression vector using NheI and EcoRI restriction sites.

Coating of screening plates

Prior to seeding, 384-well plates (PerkinElmer Life Sciences) were coated with 10% (w/v) poly-D-lysine (PDL; Sigma–Aldrich). PDL was solubilized in double-distilled H_2O. 20 μl of PDL were incubated for 1 h at room temperature and washed twice with 20 μl of PBS/well and air-dried. The coated plates were stored at 4 °C until further use.

Staining and fixation of cells

For staining of cells, Hoechst 33342 (1:1000; Life Technologies) and 3.5 μg/ml CellMask^{TM} Deep Red plasma membrane stain (Invitrogen) were added to prewarmed Dulbecco's modified Eagle's medium. 25 μl of medium/well was added to the cells and incubated for 10 min at 37 °C. Afterward, the medium was removed, and 20 μl 2% (w/v) paraformaldehyde per well were added and incubated for 20 min at room temperature. Finally, plates were washed twice with PBS and immediately used for screening.

Performance of high-content screen

HEK293 cells stably expressing EpCAM–CTF–YFP were automatically seeded (ELX406 plate washer and dispenser; BioTek, Winooski, VT; 3,000 cells in 50 μl/well) on PDL-coated 384-well plates. In the initial HCS, compounds were tested at a concentration of 8 μM (0.8% DMSO). Compound-treated cells were incubated overnight at 37 °C. Afterward, the cells were stained and fixed. The cells were imaged with the Operetta high-content imaging system (PerkinElmer Life Sciences) at 40× magnification and confocal imaging method, and the results were evaluated with the Columbus high-content imaging and analysis software version 2.8.0 (PerkinElmer Life Sciences).

Automated image analysis

Multiparametric image analysis was performed using Columbus high-content imaging and analysis software version 2.8.0 (PerkinElmer Life Sciences). The nuclei were detected via the Hoechst signal using method C of Columbus software with the following parameters: common threshold (parameter determining the lower level of pixel intensity for the whole image that may belong to nuclei), 0.30; area (to tune the merging and splitting of nuclei during nuclei detection), >30 μm^2; split factor (parameter influencing the decision of the computer whether a large object is split into two or more smaller objects or not), 7.0; individual threshold (parameter determining the intensity threshold for each object individually), 0.4; and contrast (parameter setting a lower threshold to the contrast of detected nuclei), 0.05. Method C to find nuclei provides good results for images with low background or with size variations of nuclei and supports images with large variations in intensity or contrast of nuclei.

In the next step, the area of nuclei was determined and filtered by nucleus area [μm^2] > 100. For this subpopulation called "nuclei selected," the cell mask fluorescence intensity was used to define the cytoplasm by using the building block "find cytoplasm." The building block "select cell region" was then used to distinguish membrane, nucleus and ring (cytoplasm) region. The building block "calculate intensity properties" was used to calculate the YFP intensity in the different cell compartments. In the last step, we defined five output parameters: 1) nuclei selected − number of objects; 2) nuclei selected − intensity nucleus region YFP mean − median per well; 3) nuclei selected − intensity membrane region YFP mean − median per well; 4) nuclei selected − intensity ring region YFP mean − median per well; and 5) nuclei selected − intensity cell YFP mean − median per well.

Inhibitors

Inhibition of α- and β-secretase was performed by using 3 μM GI254023X and 3 μM C3, respectively. γ-Secretase was inhibited by using 10 μM DAPT in HCS and 3 μM in membrane-based EpCAM cleavage assays.

Membrane-based EpCAM cleavage assay

These assays were performed as previously described (50, 68, 69). Briefly, the cells were treated with 20 μM compound or inhibitor overnight in assay buffer (150 mM sodium citrate, pH 6.4, 10 μM $ZnCl_2$, protease inhibitor). The cells were lysed, and the membrane fractions were generated by centrifugation steps (1,000 × g for 15 min and 16,000 × g for 20 min) and subsequently treated with 20 μM compounds or inhibitor as stated above for 22 h. The cleavage products were analyzed by SDS–PAGE and immunoblots.

Immunoblot experiments

The cells were lysed in PBS containing 1% Triton X-100 and protease inhibitors (Roche Complete). The protein concentration was determined by BCA assay (Thermo Scientific, Waltham, MA) according to the manufacturer's instructions. 20 μg of proteins were loaded onto a 12% SDS–PAGE and separated for 15 min at 15 mA and 2 h at 30 mA. Afterward, the proteins were transferred onto a methanol-equilibrated polyvinylidene difluoride blotting membrane. Visualization was done by anti-GFP antibody, in combination with a horseradish peroxidase–

conjugated secondary antibody, horseradish peroxidase substrate, and the ImageLab software version 5.2.1 (Bio-Rad).

RNA isolation, cDNA synthesis, and quantitative real-time PCR

RNA isolation was performed with the High Pure RNA isolation kit (Roche) according to the manufacturer's protocol. For removal of contaminating DNA, isolated RNA was treated twice with the Turbo DNAfree kit (Ambion, Austin, TX). Reverse transcription was done with PrimeScript™ RT Master Mix (Takara, Paris, France) according to the manufacturer's instructions. Quantitative PCR experiments were performed in a LightCycler® 480 instrument (Roche) using the KAPA SYBR Fast Universal kit according to the manufacturer's protocol. Evaluation was done by using the ΔΔcp method (70).

FACS experiments

YFP and EpCAM expression of cell lines were assessed with a BD LSR II flow cytometer (BD Biosciences). The cells were incubated with a monoclonal FITC-conjugated anti-EpCAM antibody (Life Technologies) diluted in 1× PBS (1:200) for 30 min at room temperature in the dark. Afterward, the cells were washed, resuspended in 1× PBS, and transferred to FACS measurement. The results were evaluated with the FlowJo program version 10.0.8.

Viability/cytotoxicity assay

Viability, cytotoxicity, and apoptosis of different cell lines were assessed in 384-well plates using the ApoTox Glo assay according to the manufacturer's instructions (Promega) and 5,000 cells in 50 μl of cell medium.

Proliferation assay

The cells were automatically seeded onto 96-well plates. After 6 h, one row was stained with 0.25 μl of Hoechst 33342 and imaged with Operetta high-content imaging system (PerkinElmer Life Sciences). Afterward, medium was removed, and new medium containing the compounds or DMSO or DAPT as control was added. Every 24 h, one row was stained with Hoechst 33342 and imaged (D0–D7). The results were evaluated with the program Microsoft Excel.

Author contributions—J. Y. T. and K. S. data curation; J. Y. T. and K. S. formal analysis; J. Y. T. and K. S. validation; J. Y. T., K. S., E. L., and J. T. investigation; J. Y. T. visualization; J. Y. T., O. G., and D. N. writing-original draft; J. Y. T., O. G., and D. N. writing-review and editing; K. S., K. H., O. G., and D. N. conceptualization; E. L. resources; E. L. and K. H. methodology; H.S., K. H., and D. N. supervision; K. H., O. G., and D. N. project administration; O. G. and D. N. funding acquisition.

References

1. Litvinov, S. V., Velders, M. P., Bakker, H. A., Fleuren, G. J., and Warnaar, S. O. (1994) Ep-CAM: a human epithelial antigen is a homophilic cell-cell adhesion molecule. *J. Cell Biol.* **125,** 437–446 CrossRef Medline
2. Alberti, S., Nutini, M., and Herzenberg, L. A. (1994) DNA methylation prevents the amplification of TROP1, a tumor-associated cell surface antigen gene. *Proc. Natl. Acad. Sci. U.S.A.* **91,** 5833–5837 CrossRef Medline
3. Linnenbach, A. J., Wojcierowski, J., Wu, S. A., Pyrc, J. J., Ross, A. H., Dietzschold, B., Speicher, D., and Koprowski, H. (1989) Sequence investigation of the major gastrointestinal tumor-associated antigen gene family, GA733. *Proc. Natl. Acad. Sci. U.S.A.* **86,** 27–31 CrossRef Medline
4. Szala, S., Froehlich, M., Scollon, M., Kasai, Y., Steplewski, Z., Koprowski, H., and Linnenbach, A. J. (1990) Molecular cloning of cDNA for the carcinoma-associated antigen GA733-2. *Proc. Natl. Acad. Sci. U.S.A.* **87,** 3542–3546 CrossRef Medline
5. Dollé, L., Theise, N. D., Schmelzer, E., Boulter, L., Gires, O., and van Grunsven, L. A. (2015) EpCAM and the biology of hepatic stem/progenitor cells. *Am. J. Physiol. Gastrointest. Liver Physiol.* **308,** G233–G250 CrossRef Medline
6. Schnell, U., Cirulli, V., and Giepmans, B. N. (2013) EpCAM: structure and function in health and disease. *Biochim. Biophys. Acta* **1828,** 1989–2001 CrossRef Medline
7. Baeuerle, P. A., and Gires, O. (2007) EpCAM (CD326) finding its role in cancer. *Br. J. Cancer* **96,** 417–423 CrossRef Medline
8. Litvinov, S. V., Bakker, H. A., Gourevitch, M. M., Velders, M. P., and Warnaar, S. O. (1994) Evidence for a role of the epithelial glycoprotein 40 (Ep-CAM) in epithelial cell-cell adhesion. *Cell Adhes. Commun.* **2,** 417–428 CrossRef Medline
9. Münz, M., Kieu, C., Mack, B., Schmitt, B., Zeidler, R., and Gires, O. (2004) The carcinoma-associated antigen EpCAM upregulates c-myc and induces cell proliferation. *Oncogene* **23,** 5748–5758 CrossRef Medline
10. Maetzel, D., Denzel, S., Mack, B., Canis, M., Went, P., Benk, M., Kieu, C., Papior, P., Baeuerle, P. A., Munz, M., and Gires, O. (2009) Nuclear signalling by tumour-associated antigen EpCAM. *Nat. Cell Biol.* **11,** 162–171 CrossRef Medline
11. Sankpal, N. V., Fleming, T. P., and Gillanders, W. E. (2013) EpCAM modulates NF-kappaB signaling and interleukin-8 expression in breast cancer. *Mol. Cancer Res.* **11,** 418–426 CrossRef Medline
12. Lu, T. Y., Lu, R. M., Liao, M. Y., Yu, J., Chung, C. H., Kao, C. F., and Wu, H. C. (2010) Epithelial cell adhesion molecule regulation is associated with the maintenance of the undifferentiated phenotype of human embryonic stem cells. *J. Biol. Chem.* **285,** 8719–8732 CrossRef Medline
13. Sankpal, N. V., Fleming, T. P., Sharma, P. K., Wiedner, H. J., and Gillanders, W. E. (2017) A double-negative feedback loop between EpCAM and ERK contributes to the regulation of epithelial-mesenchymal transition in cancer. *Oncogene* **36,** 3706–3717 CrossRef Medline
14. Chaves-Pérez, A., Mack, B., Maetzel, D., Kremling, H., Eggert, C., Harréus, U., and Gires, O. (2013) EpCAM regulates cell cycle progression via control of cyclin D1 expression. *Oncogene* **32,** 641–650 CrossRef Medline
15. Kuan, I. I., Liang, K. H., Wang, Y. P., Kuo, T. W., Meir, Y. J., Wu, S. C., Yang, S. C., Lu, J., and Wu, H. C. (2017) EpEX/EpCAM and Oct4 or Klf4 alone are sufficient to generate induced pluripotent stem cells through STAT3 and HIF2α. *Sci. Rep.* **7,** 41852 CrossRef Medline
16. Sarrach, S., Huang, Y., Niedermeyer, S., Hachmeister, M., Fischer, L., Gille, S., Pan, M., Mack, B., Kranz, G., Libl, D., Merl-Pham, J., Hauck, S. M., Paoluzzi Tomada, E., Kieslinger, M., Jeremias, I., *et al.* (2018) Spatiotemporal patterning of EpCAM is important for murine embryonic endo- and mesodermal differentiation. *Sci. Rep.* **8,** 1801 CrossRef Medline
17. Spizzo, G., Obrist, P., Ensinger, C., Theurl, I., Dünser, M., Ramoni, A., Gunsilius, E., Eibl, G., Mikuz, G., and Gastl, G. (2002) Prognostic significance of Ep-CAM AND Her-2/neu overexpression in invasive breast cancer. *Int. J. Cancer* **98,** 883–888 CrossRef Medline
18. Spizzo, G., Went, P., Dirnhofer, S., Obrist, P., Simon, R., Spichtin, H., Maurer, R., Metzger, U., von Castelberg, B., Bart, R., Stopatschinskaya, S., Köchli, O. R., Haas, P., Mross, F., Zuber, M., *et al.* (2004) High Ep-CAM expression is associated with poor prognosis in node-positive breast cancer. *Breast Cancer Res. Treat* **86,** 207–213 CrossRef Medline
19. Trzpis, M., McLaughlin, P. M., de Leij, L. M., and Harmsen, M. C. (2007) Epithelial cell adhesion molecule: more than a carcinoma marker and adhesion molecule. *Am. J. Pathol.* **171,** 386–395 CrossRef Medline
20. González, B., Denzel, S., Mack, B., Conrad, M., and Gires, O. (2009) Ep-CAM is involved in maintenance of the murine embryonic stem cell phenotype. *Stem Cells* **27,** 1782–1791 CrossRef Medline
21. Ng, V. Y., Ang, S. N., Chan, J. X., and Choo, A. B. (2010) Characterization of epithelial cell adhesion molecule as a surface marker on undifferentiated human embryonic stem cells. *Stem Cells* **28,** 29–35 CrossRef Medline

22. Gerlach, J. C., Foka, H. G., Thompson, R. L., Gridelli, B., and Schmelzer, E. (2018) Epithelial cell adhesion molecule fragments and signaling in primary human liver cells. *J. Cell Physiol.* **233,** 4841–4851 CrossRef Medline
23. Schmelzer, E., Zhang, L., Bruce, A., Wauthier, E., Ludlow, J., Yao, H. L., Moss, N., Melhem, A., McClelland, R., Turner, W., Kulik, M., Sherwood, S., Tallheden, T., Cheng, N., Furth, M. E., *et al.* (2007) Human hepatic stem cells from fetal and postnatal donors. *J. Exp. Med.* **204,** 1973–1987 CrossRef Medline
24. Balzar, M., Winter, M. J., de Boer, C. J., and Litvinov, S. V. (1999) The biology of the 17–1A antigen (Ep-CAM). *J. Mol. Med.* **77,** 699–712 CrossRef Medline
25. Went, P. T., Lugli, A., Meier, S., Bundi, M., Mirlacher, M., Sauter, G., and Dirnhofer, S. (2004) Frequent EpCam protein expression in human carcinomas. *Hum. Pathol.* **35,** 122–128 CrossRef Medline
26. Gires, O., Klein, C. A., and Baeuerle, P. A. (2009) On the abundance of EpCAM on cancer stem cells. *Nat. Rev. Cancer* **9,** 143 CrossRef
27. Ng, C. F., Zhou, W. J., Ng, P. K., Li, M. S., Ng, Y. K., Lai, P. B., and Tsui, S. K. (2011) Characterization of human FHL2 transcript variants and gene expression regulation in hepatocellular carcinoma. *Gene* **481,** 41–47 CrossRef Medline
28. Gosens, M. J., van Kempen, L. C., van de Velde, C. J., van Krieken, J. H., and Nagtegaal, I. D. (2007) Loss of membranous Ep-CAM in budding colorectal carcinoma cells. *Mod. Pathol.* **20,** 221–232 CrossRef Medline
29. Yanamoto, S., Kawasaki, G., Yoshitomi, I., Iwamoto, T., Hirata, K., and Mizuno, A. (2007) Clinicopathologic significance of EpCAM expression in squamous cell carcinoma of the tongue and its possibility as a potential target for tongue cancer gene therapy. *Oral Oncol.* **43,** 869–877 CrossRef Medline
30. Ralhan, R., Cao, J., Lim, T., Macmillan, C., Freeman, J. L., and Walfish, P. G. (2010) EpCAM nuclear localization identifies aggressive thyroid cancer and is a marker for poor prognosis. *BMC Cancer* **10,** 331 CrossRef Medline
31. Ralhan, R., He, H. C., So, A. K., Tripathi, S. C., Kumar, M., Hasan, M. R., Kaur, J., Kashat, L., MacMillan, C., Chauhan, S. S., Freeman, J. L., and Walfish, P. G. (2010) Nuclear and cytoplasmic accumulation of Ep-ICD is frequently detected in human epithelial cancers. *PLoS One* **5,** e14130 CrossRef Medline
32. Brunner, A., Prelog, M., Verdorfer, I., Tzankov, A., Mikuz, G., and Ensinger, C. (2008) EpCAM is predominantly expressed in high grade and advanced stage urothelial carcinoma of the bladder. *J. Clin. Pathol.* **61,** 307–310 Medline
33. Fong, D., Steurer, M., Obrist, P., Barbieri, V., Margreiter, R., Amberger, A., Laimer, K., Gastl, G., Tzankov, A., and Spizzo, G. (2006) Ep-CAM expression in pancreatic and ampullary carcinomas: frequency and prognostic relevance. *J. Clin. Pathol.*
34. Kim, M. Y., Oskarsson, T., Acharyya, S., Nguyen, D. X., Zhang, X. H., Norton, L., and Massagué, J. (2009) Tumor self-seeding by circulating cancer cells. *Cell* **139,** 1315–1326 CrossRef Medline
35. Massoner, P., Thomm, T., Mack, B., Untergasser, G., Martowicz, A., Bobowski, K., Klocker, H., Gires, O., and Puhr, M. (2014) EpCAM is overexpressed in local and metastatic prostate cancer, suppressed by chemotherapy and modulated by MET-associated miRNA-200c/205. *Br. J. Cancer* **111,** 955–964 CrossRef Medline
36. Später, D., Hansson, E. M., Zangi, L., and Chien, K. R. (2014) How to make a cardiomyocyte. *Development* **141,** 4418–4431 CrossRef Medline
37. van der Gun, B. T., Melchers, L. J., Ruiters, M. H., de Leij, L. F., McLaughlin, P. M., and Rots, M. G. (2010) EpCAM in carcinogenesis: the good, the bad or the ugly. *Carcinogenesis* **31,** 1913–1921 CrossRef Medline
38. Varga, M., Obrist, P., Schneeberger, S., Mühlmann, G., Felgel-Farnholz, C., Fong, D., Zitt, M., Brunhuber, T., Schäfer, G., Gastl, G., and Spizzo, G. (2004) Overexpression of epithelial cell adhesion molecule antigen in gallbladder carcinoma is an independent marker for poor survival. *Clin. Cancer Res.* **10,** 3131–3136 CrossRef Medline
39. Park, S. Y., Bae, J. S., Cha, E. J., Chu, H. H., Sohn, J. S., and Moon, W. S. (2016) Nuclear EpICD expression and its role in hepatocellular carcinoma. *Oncol. Rep.* **36,** 197–204 CrossRef Medline
40. Went, P., Dirnhofer, S., Salvisberg, T., Amin, M. B., Lim, S. D., Diener, P. A., and Moch, H. (2005) Expression of epithelial cell adhesion molecule (EpCam) in renal epithelial tumors. *Am. J. Surg. Pathol.* **29,** 83–88 CrossRef Medline
41. Zheng, X., Fan, X., Fu, B., Zheng, M., Zhang, A., Zhong, K., Yan, J., Sun, R., Tian, Z., and Wei, H. (2017) EpCAM inhibition sensitizes chemoresistant leukemia to immune surveillance. *Cancer Res.* **77,** 482–493 CrossRef Medline
42. Wenqi, D., Li, W., Shanshan, C., Bei, C., Yafei, Z., Feihu, B., Jie, L., and Daiming, F. (2009) EpCAM is overexpressed in gastric cancer and its downregulation suppresses proliferation of gastric cancer. *J. Cancer Res. Clin. Oncol.* **135,** 1277–1285 CrossRef Medline
43. Gires, O. (2008) TACSTD1 (tumor-associated calcium signal transducer 1). *Atlas Genet. Cytogenet. Oncol. Haematol.* http://atlasgeneticsoncology.org/Genes/TACSTD1ID42459ch2p21.html
44. Munz, M., Baeuerle, P. A., and Gires, O. (2009) The emerging role of EpCAM in cancer and stem cell signaling. *Cancer Res.* **69,** 5627–5629 CrossRef Medline
45. Strnad, J., Hamilton, A. E., Beavers, L. S., Gamboa, G. C., Apelgren, L. D., Taber, L. D., Sportsman, J. R., Bumol, T. F., Sharp, J. D., and Gadski, R. A. (1989) Molecular cloning and characterization of a human adenocarcinoma/epithelial cell surface antigen complementary DNA. *Cancer Res.* **49,** 314–317 Medline
46. Chong, J. M., and Speicher, D. W. (2001) Determination of disulfide bond assignments and *N*-glycosylation sites of the human gastrointestinal carcinoma antigen GA733-2 (CO17–1A, EGP, KS1–4, KSA, and Ep-CAM). *J. Biol. Chem.* **276,** 5804–5813
47. Molina, F., Bouanani, M., Pau, B., and Granier, C. (1996) Characterization of the type-1 repeat from thyroglobulin, a cysteine-rich module found in proteins from different families. *Eur. J. Biochem.* **240,** 125–133 CrossRef Medline
48. Denzel, S., Maetzel, D., Mack, B., Eggert, C., Bärr, G., and Gires, O. (2009) Initial activation of EpCAM cleavage via cell-to-cell contact. *BMC Cancer* **9,** 402 CrossRef Medline
49. Edwards, D. R., Handsley, M. M., and Pennington, C. J. (2008) The ADAM metalloproteinases. *Mol. Aspects Med.* **29,** 258–289 CrossRef Medline
50. Tsaktanis, T., Kremling, H., Pavsic, M., von Stackelberg, R., Mack, B., Fukumori, A., Steiner, H., Vielmuth, F., Spindler, V., Huang, Z., Jakubowski, J., Stoecklein, N. H., Luxenburger, E., Lauber, K., Lenarcic, B., *et al.* (2015) Cleavage and cell adhesion properties of human epithelial cell adhesion molecule (HEPCAM). *J. Biol. Chem.* **290,** 24574–24591 CrossRef Medline
51. Barolo, S. (2006) Transgenic Wnt/TCF pathway reporters: all you need is Lef? *Oncogene* **25,** 7505–7511 CrossRef Medline
52. Imrich, S., Hachmeister, M., and Gires, O. (2012) EpCAM and its potential role in tumor-initiating cells. *Cell Adh. Migr.* **6,** 30–38 CrossRef Medline
53. Maaser, K., and Borlak, J. (2008) A genome-wide expression analysis identifies a network of EpCAM-induced cell cycle regulators. *Br. J. Cancer* **99,** 1635–1643 CrossRef Medline
54. Münz, M., Murr, A., Kvesic, M., Rau, D., Mangold, S., Pflanz, S., Lumsden, J., Volkland, J., Fagerberg, J., Riethmüller, G., Ruttinger, D., Kufer, P., Baeuerle, P. A., and Raum, T. (2010) Side-by-side analysis of five clinically tested anti-EpCAM monoclonal antibodies. *Cancer Cell Int.* **10,** 44 CrossRef Medline
55. Riesenberg, R., Buchner, A., Pohla, H., and Lindhofer, H. (2001) Lysis of prostate carcinoma cells by trifunctional bispecific antibodies (αEpCAM × αCD3). *J. Histochem. Cytochem.* **49,** 911–917 CrossRef Medline
56. Groth, A., Salnikov, A. V., Ottinger, S., Gladkich, J., Liu, L., Kallifatidis, G., Salnikova, O., Ryschich, E., Giese, N., Giese, T., Momburg, F., Büchler, M. W., Moldenhauer, G., and Herr, I. (2012) New gene-immunotherapy combining TRAIL-lymphocytes and EpCAMxCD3 bispecific antibody for tumor targeting. *Clin. Cancer Res.* **18,** 1028–1038 CrossRef Medline
57. Neighbors, M., Apt, D., Chang, J. C., Brinkman, A., Sipos-Solman, I., Ong, R., Leong, S., and Punnonen, J. (2008) EpCAM-specific vaccine response by modified antigen and chimeric costimulatory molecule in cynomolgus monkeys. *J. Immunother.* **31,** 644–655 CrossRef Medline
58. Waldron, N. N., Barsky, S. H., Dougherty, P. R., and Vallera, D. A. (2014) A bispecific EpCAM/CD133-targeted toxin is effective against carcinoma. *Target Oncol.* **9,** 239–249 CrossRef Medline

59. Lund, K., Bostad, M., Skarpen, E., Braunagel, M., Kiprijanov, S., Krauss, S., Duncan, A., Høgset, A., and Selbo, P. K. (2014) The novel EpCAM-targeting monoclonal antibody 3–17I linked to saporin is highly cytotoxic after photochemical internalization in breast, pancreas and colon cancer cell lines. *MAbs* **6,** 1038–1050 CrossRef Medline
60. Schmohl, J. U., Felices, M., Todhunter, D., Taras, E., Miller, J. S., and Vallera, D. A. (2016) Tetraspecific scFv construct provides NK cell mediated ADCC and self-sustaining stimuli via insertion of IL-15 as a cross-linker. *Oncotarget* **7,** 73830–73844 Medline
61. Sears, H. F., Atkinson, B., Mattis, J., Ernst, C., Herlyn, D., Steplewski, Z., Hayry, P., and Koprowski, H. (1982) Phase-I clinical trial of monoclonal antibody in treatment of gastrointestinal tumours. *Lancet* **1,** 762–765 24461749, 2564569, 2895283, 2895282, 2895281, 2895280, 2858033, 6132102, 6132101, 6121224, 6110961, 6110960, 6103172, 6103171, 85998, 85997, 47998, 4132507, 4132506, 4120735
62. Sears, H. F., Herlyn, D., Steplewski, Z., and Koprowski, H. (1984) Effects of monoclonal antibody immunotherapy on patients with gastrointestinal adenocarcinoma. *J. Biol. Response Mod.* **3,** 138–150 Medline
63. Fields, A. L., Keller, A., Schwartzberg, L., Bernard, S., Kardinal, C., Cohen, A., Schulz, J., Eisenberg, P., Forster, J., and Wissel, P. (2009) Adjuvant therapy with the monoclonal antibody Edrecolomab plus fluorouracil-based therapy does not improve overall survival of patients with stage III colon cancer. *J. Clin. Oncol.* **27,** 1941–1947 CrossRef Medline
64. Schmoll, H. J., and Arnold, D. (2009) When wishful thinking leads to a misty-eyed appraisal: the story of the adjuvant colon cancer trials with edrecolomab. *J. Clin. Oncol.* **27,** 1926–1929 CrossRef Medline
65. Linke, R., Klein, A., and Seimetz, D. (2010) Catumaxomab: clinical development and future directions. *MAbs* **2,** 129–136 CrossRef Medline
66. Liao, M. Y., Lai, J. K., Kuo, M. Y., Lu, R. M., Lin, C. W., Cheng, P. C., Liang, K. H., and Wu, H. C. (2015) An anti-EpCAM antibody EpAb2-6 for the treatment of colon cancer. *Oncotarget* **6,** 24947–24968 CrossRef Medline
67. Oishi, N., Yamashita, T., and Kaneko, S. (2014) Molecular biology of liver cancer stem cells. *Liver Cancer* **3,** 71–84 CrossRef Medline
68. Hachmeister, M., Bobowski, K. D., Hogl, S., Dislich, B., Fukumori, A., Eggert, C., Mack, B., Kremling, H., Sarrach, S., Coscia, F., Zimmermann, W., Steiner, H., Lichtenthaler, S. F., and Gires, O. (2013) Regulated intramembrane proteolysis and degradation of murine epithelial cell adhesion molecule mEpCAM. *PLoS One* **8,** e71836 CrossRef Medline
69. Sastre, M., Steiner, H., Fuchs, K., Capell, A., Multhaup, G., Condron, M. M., Teplow, D. B., and Haass, C. (2001) Presenilin-dependent γ-secretase processing of β-amyloid precursor protein at a site corresponding to the S3 cleavage of Notch. *EMBO Rep.* **2,** 835–841 CrossRef Medline
70. Pfaffl, M. W. (2001) A new mathematical model for relative quantification in real-time RT–PCR. *Nucleic Acids Res.* **29,** e45 CrossRef Medline
71. Zhang, J. H., Chung, T. D., and Oldenburg, K. R. (1999) A simple statistical parameter for use in evaluation and validation of high throughput screening assays. *J. Biomol. Screen* **4,** 67–73 CrossRef Medline

A high-content screen for small-molecule regulators of epithelial cell-adhesion molecule (EpCAM) cleavage yields a robust inhibitor

Jana Ylva Tretter, Kenji Schorpp, Elke Luxenburger, Johannes Trambauer, Harald Steiner, Kamyar Hadian, Olivier Gires and Dierk Niessing

J. Biol. Chem. 2018, 293:8994-9005.
doi: 10.1074/jbc.RA118.002776 originally published online April 26, 2018